Living and Syndioselective Polymerization of Methacrylates by Constrained Geometry Titanium Alkyl and Enolate Complexes

Antonio Rodriguez-Delgado, Wesley R. Mariott, and Eugene Y.-X. Chen*

Department of Chemistry, Colorado State University, Fort Collins, Colorado 80523-1872

Received February 2, 2004; Revised Manuscript Received February 25, 2004

ABSTRACT: This paper reports the homopolymerization and block copolymerization of methacrylates by the cationic titanium methyl complex, CGCTiMe$^+$MeB$(C_6F_5)_3^-$ (**1**, CGC = $Me_2Si(Me_4C_5)(t\text{-BuN})$), as well as the synthesis and methyl methacrylate (MMA) polymerization of three new neutral and cationic CGC Ti ester enolate complexes. Unlike the isostructural, cationic CGC Zr methyl complex, which is inactive for polymerization of MMA, CGC Ti methyl complex **1** effects living polymerizations of MMA and BMA (BMA = *n*-butyl methacrylate) at ambient temperature, producing syndiotactic PMMA ([rr] = 82%, P_r = 0.90) and PBMA ([rr] = 89%, P_r = 0.95). Sequential copolymerization using **1** and starting from either MMA or BMA produces the well-defined, syndiotactic diblock copolymer PMMA-*b*-PBMA with narrow molecular weight distribution (M_w/M_n = 1.08). On the other hand, copolymerizing MMA and BMA simultaneously affords the homogeneous random copolymer PMMA-*co*-PBMA. Two neutral CGC Ti ester enolate complexes, CGCTiCl[OC(O^{i}Pr)═CMe$_2$] (**2**) and CGCTiMe[OC(O^{i}Pr)═CMe$_2$] (**4**), have been synthesized, and the molecular structure of **4** has been determined by X-ray crystallography. The reaction of **4** and $B(C_6F_5)_3$·THF (THF = tetrahydrofuran) in methylene chloride readily generates the cationic CGC Ti ester enolate complex, CGCTi$^+$(THF)[OC(O^{i}Pr)═CMe$_2$] [MeB$(C_6F_5)_3]^-$ (**5**). All three CGC Ti ester enolate complexes have been investigated for MMA polymerization; of particular interest are the polymer characteristics (molecular weight, molecular weight distribution, and syndiotacticity) of the PMMA formed by **5**, which are remarkably similar to those of the PMMA by **1**, suggesting that the cationic ester enolate **5** is an appropriate model for the propagating species involved in the MMA polymerization by the alkyl cation **1**. The microstructures of PMMA have been analyzed at the pentad level, and the polymerization mechanism has also been discussed.

Introduction

Metallocene-mediated methyl methacrylate (MMA) polymerization marked its beginning with three independent reports of the effective MMA polymerization metallocene complexes: chloro-metallocene enolates $Cp_2MCl[OC(OMe)═CMe_2]$ (M = Zr, Ti) by Farnham and Hertler,[1] lanthanocenes such as $(C_5Me_5)_2SmMe(THF)$ by Yasuda et al.,[2] and zirconocene dimethyl Cp_2ZrMe_2 (in combination with zirconocenium activator $[Cp_2ZrMe(THF)]^+[BPh_4]^-$) by Collins and Ward.[3] Specifically regarding the intensively investigated zirconocene-mediated MMA polymerization, Collins and co-workers subsequently showed that a two-component system, which consists of a neutral zirconocene ester enolate initiator such as $Cp_2ZrMe[OC(Ot\text{Bu})═CMe_2]$ and a cationic catalyst such as $[Cp_2Zr(THF)Me]^+[BPh_4]^-$, polymerizes MMA in a living fashion to syndiotactic rich poly(methyl methacrylate) (PMMA).[4] This polymerization follows a group-transfer-type[5] bimetallic propagating mechanism.[4a,6] For MMA polymerization mediated by single-component, bridged (*ansa*-) zirconocenium complexes, however, a *monometallic*, 1,4-conjugated addition pathway that involves a cationic *ansa*-zirconocene ester enolate propagating species has been proposed.[7] This propagation mechanism is similar to that proposed for MMA polymerization mediated by the isoelectronic, neutral lanthanocenes.[8]

Three recent reports[7a,9,10] investigated the synthesis of block copolymers of methacrylates utilizing the living nature of the zirconocene-mediated methacrylate polymerization. We reported the synthesis of isotactic-*b*-syndiotactic stereodiblock PMMA starting from the construction of the isotactic block using the chiral *ansa*-zirconocenium cation.[7a] Most recently, Hadjichristidis and co-workers reported the synthesis of well-defined block copolymer PBMA-*b*-PMMA [PBMA = poly(*n*-butyl methacrylate)] using a three-component initiator system composed of a metallocene dimethyl, a borane or borate cocatalyst, and a large excess of $ZnEt_2$.[9] The order of monomer addition is critical in this sequential block copolymerization; if MMA was first polymerized followed by BMA, a mixture of homopolymers resulted. Additionally, Gibson et al. showed that, if a single, achiral cationic zirconocene alkyl complex was used, it did not allow block copolymerization of methacrylates.[10]

As compared to the intensively investigated MMA polymerization by zirconocenes, MMA polymerization by *titanocenes* drew much less attention. Titanocene dichloride Cp_2TiCl_2 (plus excess $AlEt_3$) was used to copolymerize MMA and acrylonitrile with a proposed ionic coordination mechanism.[11] Farnham and Hertler used $Cp_2TiCl[OC(OMe)═CMe_2]$ to polymerize MMA, affording PMMA with polydispersity index (PDI) ranging from 3.14 to 4.30.[1] Saegusa and co-workers employed similar titanocene mono- or bis-enolates, but combined them with activators such as $AgN(SO_2CF_3)_2$ and $[PhNHMe_2]^+[B(C_6F_5)_4]^-$, affording PMMA with PDI ranging from 2.1 to 2.5.[12] Most recently, Marks and co-workers reported that a three-component initiator system composed of $(C_5Me_5)TiMe_3$, $Ph_3C^+[B(C_6F_5)_4]^-$, and Zn is also effective for MMA polymerization, producing syndiotactic PMMA with racemic triad [rr] ∼ 70% and PDI ∼ 2.0.[13] Exploring group 4 metallocenes for polymerization of other functionalized olefinic monomers, Erker and co-workers showed that the $B(C_6F_5)_3$ adducts of titanocene (and zirconocene) ketone enolates are effective initiators for polymerization of methyl vinyl ketone.[14]

We have been investigating MMA homopolymerization[15] and block copolymerization with propylene[16] using

10.1021/ma049774g CCC: $27.50
Published on Web 04/06/2004

Chart 1

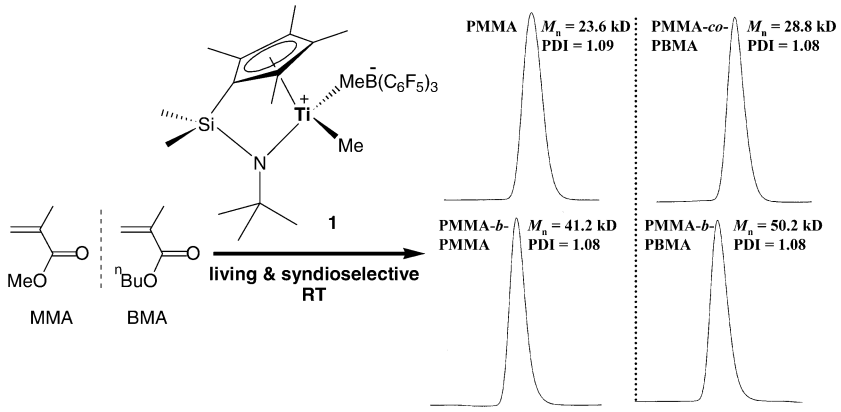

ansa-titanocenes and related complexes such as chiral *ansa*-titanocene imido complexes[15a] and a technologically significant olefin-polymerization constrained geometry catalyst[17]—$CGCTiMe_2$ [CGC = $Me_2Si(Me_4C_5)(t\text{-}BuN)$].[17o] The central objective of this investigation is to study titanocene initiators that can effect living and stereospecific polymerization of alkyl methacrylates, for the synthesis of well-defined stereoregular block copolymers and a understanding of the propagating species responsible for the polymerization activity and stereoregulation. We report here the first living polymerization of alkyl methacrylates initiated by a cationic titanium alkyl complex—$CGCTiMe^+MeB(C_6F_5)_3^-$ (**1**), Chart 1.[18] Titanium methyl cation **1** effects *living* polymerization of MMA and BMA at room temperature (RT), producing *syndiotactic* PMMA ([rr] = 82%, P_r = 0.90) and PBMA ([rr] = 89%, P_r = 0.95). The living nature of this polymerization allows for the synthesis of the well-defined syndiotactic diblock copolymer of MMA and BMA with a small PDI value of 1.08 via sequential copolymerization starting from either MMA *or* BMA. The syndiotactic random copolymer can also be prepared from the one-pot copolymerization. The study of the independently synthesized CGC Ti ester enolates indicates the cationic CGC Ti ester enolate is a suitable model for the propagating species involved in MMA polymerization by complex **1**.

Experimental Section

Materials and Methods. All syntheses and manipulations of air- and moisture-sensitive materials were carried out in flamed Schlenk-type glassware on a dual-manifold Schlenk line, on a high-vacuum line (10^{-5} to 10^{-7} Torr), or in an argon-filled glovebox (<1.0 ppm oxygen and moisture). NMR-scale reactions (typically in a 0.02 mmol scale) were conducted in Teflon-valve-sealed J. Young-type NMR tubes. HPLC grade organic solvents were first saturated with nitrogen during filling of the solvent reservoir and then dried by passage through activated alumina (for diethyl ether, tetrahydrofuran (THF), and methylene chloride) followed by passage through Q-5 supported copper catalyst (for toluene and hexanes) stainless steel columns. Benzene-d_6, toluene-d_8, and THF-d_8 were dried over sodium/potassium alloy and vacuum-distilled or filtered, whereas CD_2Cl_2 and $CDCl_3$ were dried over activated Davison 4 Å molecular sieves. NMR spectra were recorded on either a Varian Inova 300 (FT 300 MHz, ^{1}H; 75 MHz, ^{13}C; 282 MHz, ^{19}F) or a Varian Inova 400 spectrometer. Chemical shifts for ^{1}H and ^{13}C spectra were referenced to internal solvent resonances and are reported as parts per million relative to tetramethylsilane, whereas ^{19}F NMR spectra were referenced to external $CFCl_3$. Elemental analyses were performed by Desert Analytics, Tucson, AZ.

Isobutyric acid, thionyl chloride, *n*-BuLi (1.6 M in hexanes), and MeMgBr (3.0 M in diethyl ether) were purchased from Aldrich Chemical Co. and used as received. Trimethylaluminum (neat) was purchased from Strem Chemical Co. and methyllithium (1.6 M in diethyl ether) from Acros.

Methyl methacrylate (MMA) and *n*-butyl methacrylate (BMA) were purchased from Aldrich Chemical Co.; both monomers were first degassed and dried over CaH_2 overnight, followed by vacuum distillation. Final purification involved titration with neat tri(*n*-octyl)aluminum to a yellow end point[19] followed by distillation under reduced pressure. The purified monomers were stored in a −30 °C freezer inside the glovebox.

Tris(pentafluorophenyl)borane, $B(C_6F_5)_3$, was obtained as a research gift from Boulder Scientific Co. and further purified by recrystallization from hexanes at −30 °C. The borane−THF adduct, $B(C_6F_5)_3{\cdot}THF$, was prepared by addition of THF to a toluene solution of the borane followed by removing the solvents and drying in vacuo. $Me_2Si(C_5Me_4)(^tBuN)TiMe_2$ ($CGCTiMe_2$),[17o] $CGCTiMe^+MeB(C_6F_5)_3^-$ (**1**),[20] and lithium isopropylisobutyrate [Li(IPIB)][21] were prepared according to literature procedures.

Synthesis of $CGCTiCl[OC(O^iPr){=}CMe_2]$ (2). In an argon-filled glovebox, a 50 mL flame-dried Schlenk flask was equipped with a magnetic stir bar and charged with $CGCTiCl_2$ (0.30 g, 0.81 mmol) and 20 mL of THF. The flask was removed from the glovebox, interfaced to a Schlenk line, and cooled to −70 °C. To this flask was added a 10 mL THF solution of $LiOC(O^iPr){=}CMe_2$ (0.14 g, 1.05 mmol). The reaction mixture was allowed to warm slowly to ambient temperature and stirred for 14 h, upon which time the solution turned from bright yellow to dark red. Volatiles were removed in vacuo to give a dark red oily residue. The flask was brought back into the glovebox, and 20 mL of hexanes was added. The resulting suspension was filtered through a pad of Celite, and the solvent of the red filtrate was removed under reduced pressure to produce 0.30 g of the crude product as a sticky oil. Recrystallization of this crude material from hexanes at −30 °C yielded 0.24 g (64%) of the pure complex **2** as an orange-red microcrystalline solid. Anal. Calcd. for $C_{22}H_{40}NO_2SiClTi$: C, 57.19; H, 8.73; N, 3.03. Found: C, 57.33; H, 8.66; N, 3.30.

^{1}H NMR (C_6D_6, 23 °C) for $Me_2Si(Me_4C_5)(t\text{-}BuN)TiCl[OC(O^iPr){=}CMe_2]$ (**2**): δ 4.61 (sept, J = 6.0 Hz, 1H, C*H*Me_2), 2.25 (s, 3H, C_5Me_4), 2.08 (s, 3H, C_5Me_4), 2.03 (s, 3H, C_5Me_4), 1.90 (s, 3H, C_5Me_4), 1.80 (s, 3H, ═CMe_2), 1.77 (s, 3H, ═CMe_2), 1.39 (s, 9H, *t*Bu), 1.24 (d, J = 6.3 Hz, 3H, OCMe_2), 1.18 (d, J = 6.0 Hz, 3H, OCMe_2), 0.56 (s, 3H, SiMe_2), 0.51 (s, 3H, SiMe_2). ^{13}C NMR (C_6D_6, 23 °C): δ 154.3 ((TiO*C*), 136.81, 135.37, 132.27, 102.3 (C_5Me_4), 89.83 (═*C*Me_2), 69.56 (O*C*Me_2), 60.44 (N*C*Me_3), 32.57 (NCMe_3), 22.36 (OCMe_2), 21.50 (OCMe_2), 17.88 (═CMe_2), 17.13 (═CMe_2), 15.66 (C_5Me_4), 14.46 (C_5Me_4), 12.77 (C_5Me_4), 10.23 (C_5Me_4), 6.28 (SiMe_2), 5.62 (SiMe_2).

Synthesis of CGCTiMeCl (3). In an argon-filled glovebox, a 30 mL glass reactor was equipped with a magnetic stir bar, charged with **2** (0.20 g, 0.43 mmol) followed by 20 mL of toluene, and wrapped with aluminum foil. To this reactor, with vigorous stirring, was added 0.51 mL of $AlMe_3$ (0.99 M in hexanes, 0.51 mmol). The reaction mixture was stirred at ambient temperature for 14 h, upon which time the mixture turned from red orange to brownish yellow. Volatiles were

removed in vacuo to give the crude product as a brownish oil; recrystallization of this crude material from hexanes at −30 °C yielded 0.11 g (89%) of the pure complex **3** as a yellow microcrystalline solid. Anal. Calcd for $C_{16}H_{30}NSiClTi$: C, 55.24; H, 8.69; N, 4.03. Found: C, 54.93; H, 8.47; N, 3.73.

^{1}H NMR (C_6D_6, 23 °C) for $Me_2Si(Me_4C_5)$(*t*-BuN)TiMeCl (**3**): δ 2.00 (s, 3H, C_5Me_4), 1.99 (s, 3H, C_5Me_4), 1.91 (s, 3H, C_5Me_4), 1.88 (s, 3H, C_5Me_4), 1.50 (s, 9H, *t*Bu), 0.85 (s, 3H, Ti*Me*), 0.45 (s, 3H, SiMe_2), 0.36 (s, 3H, SiMe_2). ^{13}C NMR (C_6D_6, 23 °C): δ 136.29, 134.35, 133.23, 101.5 (C_5Me_4), 59.39 (N*C*Me_3), 53.13 (Ti*Me*), 33.69 (NC*Me*$_3$), 15.28 (C_5Me_4), 14.90 (C_5Me_4), 12.48 (C_5Me_4), 11.89 (C_5Me_4), 5.67 (SiMe_2), 5.61 (SiMe_2).

Synthesis of CGCTiMe[OC(O^{i}Pr)═CMe$_2$] (4). In an argon-filled glovebox, a 20 mL reactor was equipped with a magnetic stir bar and charged with **3** (0.15 g, 0.43 mmol) in 10 mL of toluene followed by addition of a 10 mL toluene solution of LiOC(O^{i}Pr)═CMe_2, (0.105 g, 0.78 mmol). The flask was wrapped with aluminum foil, and the reaction mixture was stirred for 16 h at ambient temperature. Volatiles were removed in vacuo to give an orange oil, and 20 mL of hexanes was added to precipitate LiCl. The resulting suspension was filtered through a pad of Celite, and the solvent of the filtrate was removed under reduced pressure to give the crude product as a yellow oil. Recrystallization of the crude product from hexanes at −30 °C yielded 0.11 g (58%) of the pure complex **4** as yellow crystals. These crystals were suitable for X-ray diffraction analysis; thus, complex **4** was characterized by X-ray crystallography (vide infra).

^{1}H NMR (C_6D_6, 23 °C) for $Me_2Si(Me_4C_5)$(*t*-BuN)TiMe[OC(O^{i}Pr)═CMe_2] (**4**): δ 4.32 (sept, J = 6.0 Hz, 1H, C*H*Me_2), 2.16 (s, 3H, C_5Me_4), 2.06 (s, 3H, C_5Me_4), 1.92 (s, 3H, C_5Me_4), 1.79 (s, 3H, C_5Me_4), 1.83 (s, 3H, ═CMe_2), 1.74 (s, 3H, ═CMe_2), 1.40 (s, 9H, *t*Bu), 1.20 (d, J = 2.4 Hz, 3H, OCMe_2), 1.18 (d, J = 2.4 Hz, 3H, OCMe_2), 0.53 (s, 3H, SiMe_2), 0.52 (s, 3H, Ti*Me*), 0.51-(s, 3H, SiMe_2). ^{1}H NMR (CD_2Cl_2, 23 °C): δ 4.15 (sept, J = 6.0 Hz, 1H, C*H*Me_2), 2.15 (s, 3H, C_5Me_4), 2.04 (s, 3H, C_5Me_4), 2.02 (s, 3H, C_5Me_4), 1.79 (s, 3H, C_5Me_4), 1.55 (s, 3H, ═CMe_2), 1.52 (s, 3H, ═CMe_2), 1.31 (s, 9H, *t*Bu), 1.13 (s br, 3H, OCMe_2), 1.11 (s br, 3H, OCMe_2), 0.53 (s, 3H, SiMe_2), 0.51(s, 3H, SiMe_2), 0.13 (s, 3H, Ti*Me*). ^{13}C NMR (C_6D_6, 23 °C): δ 154.7 (TiO*C*-), 131.81, 131.59, 130.24, 101.64 (C_5Me_4), 88.31 (═*C*Me_2), 68.41 (O*C*Me_2), 58.22 (N*C*Me_3), 40.66 (Ti*Me*), 33.72 (NC*Me*$_3$), 22.12 (OC*Me*$_2$), 21.79 (OC*Me*$_2$), 17.88 (═C*Me*$_2$), 17.18 (═C*Me*$_2$), 15.13 (C_5Me_4), 14.32 (C_5Me_4), 11.84 (C_5Me_4), 9.84 (C_5Me_4), 6.52 (SiMe_2), 5.89 (SiMe_2).

VT NMR Experiments for in Situ Generation of CGCTi$^+$(THF)[OC(O^{i}Pr)═CMe$_2$] [MeB(C$_6$F$_5$)$_3$]$^-$ (5). In an argon-filled glovebox, a Teflon-valve-sealed J. Young-type NMR tube was charged with **4** (8.8 mg, 0.02 mmol) and B(C_6F_5)$_3$·THF (11.7 mg, 0.02 mmol). The NMR tube was removed from the glovebox, interfaced to a high vacuum line, and degassed at ambient temperature. A separate vacuum tube was charged with CD_2Cl_2 and degassed at −78 °C; approximately 0.7 mL of CD_2Cl_2 was condensed into the NMR tube at −78 °C to give an orange suspension which, upon gentle shacking, formed an orange red homogeneous solution. The NMR tube was detached from the high vacuum line and kept in a −78 °C bath before the NMR experiments. The formation of the red solution upon mixing **4** and B(C_6F_5)$_3$·THF indicated the reaction took place even at −78 °C. The reaction was monitored by ^{1}H and ^{19}F NMR spectroscopy starting from a precooled probe temperature of −60 °C and ending at 23 °C. Indeed, this reaction was already complete within 15 min on going from −78 to −60 °C, with the observed spectroscopic data being consistent with the structure of the cationic ester enolate complex **5**. Upon warming to above −40 °C, despite evidence of minor decomposition, complex **5** largely preserved, even after 4 h at 23 °C. The use of a stoichiometric amount of THF (from B(C_6F_5)$_3$·THF) was critical for the direct observation of the cationic ester enolate complex; the reaction of **4** with B(C_6F_5)$_3$ in CD_2Cl_2 gave a mixture of products even at −60 °C.

^{1}H NMR (CD_2Cl_2, 23 °C) for $Me_2Si(Me_4C_5)$(*t*-BuN)Ti$^+$-(THF)[OC(O^{i}Pr)═CMe_2][MeB(C_6F_5)$_3$]$^-$ (**5**): δ 4.09 (sept, J = 4.5 Hz, 1H, C*H*Me_2), 3.78 (m, 4H, CH_2CH_2), 2.23 (s, 3H, C_5Me_4), 2.11 (s, 3H, C_5Me_4), 2.10 (s, 3H, C_5Me_4), 2.09 (s, 3H, C_5Me_4), 1.93 (m, 4H, CH_2CH_2), 1.67 (s, 3H, ═CMe_2), 1.64 (s, 3H, ═CMe_2), 1.29 (s, 9H, *t*Bu), 1.21 (d, J = 2.1 Hz, 3H, OCMe_2), 1.18 (d, J = 2.1 Hz, 3H, OCMe_2), 0.86 (s, 3H, SiMe_2), 0.82 (s, 3H, SiMe_2), 0.46 (s br, 3H, B*Me*). ^{19}F NMR (CD_2Cl_2, 23 °C): δ −131.60 (d, $^3J_{F-F}$ = 22.6 Hz, 6F, *o*-F), −163.66 (t, $^3J_{F-F}$ = 20.9 Hz, 3F, *p*-F), −166.27 (m, 6F, *m*-F).

Table 1. Crystal Data and Structure Refinements for 4

empirical formula	$C_{23}H_{43}NO_2SiTi$
formula weight	441.57
temp/K	173(2)
wavelength/Å	0.710 73
cryst syst	monoclinic
space group	$P2_1/n$
a/Å	15.212(3)
b/Å	9.1575(19)
c/Å	18.012(4)
α/deg	90
β/deg	90.050(4)
γ/deg	90
vol/Å3	2509.1(9)
Z	4
density (calcd)/(mg/m^3)	1.169
abs coeff/mm^{-1}	0.406
F(000)	960
cryst size/mm^3	0.40 × 0.20 × 0.18
q range for data collection/deg	1.75−32.26
index ranges	$-16 \le h \le 16$, $-10 \le k \le 10$, $-20 \le l \le 20$
reflecns collected	15 551
independ reflecns	3613 [R_{int} = 0.0655]
data/restraints/params	3613/0/254
goodness-of-fit on F^2	1.007
final R indices [$I > 2\sigma(I)$]	R_1 = 0.0537, R_{w2} = 0.1378
R indices (all data)	R_1 = 0.0683, R_{w2} = 0.1488
extinction coeff	0.0095(13)
largest diff. peak and hole/(e Å^{-3})	0.501 and −0.494

X-ray Crystallographic Analysis of 4. Single crystals suitable for X-ray diffraction studies were obtained by slow recrystallization from hexanes at −30 °C. After the mother liquor was decanted in the glovebox, the crystals were quickly covered with a layer of Paratone-N oil (Exxon, dried and degassed at 120 °C/(10^{-6} Torr) for 24 h), mounted on thin glass fibers, and transferred into the cold nitrogen steam of a Siemens SMART CCD diffractometer. The structures were solved by direct methods and refined using the Siemens SHELXTL program library.[22] The structures were refined by full matrix weighted least-squares on F^2 for all reflections. All non-hydrogen atoms were refined with anisotropic displacement parameters, whereas hydrogen atoms were included in the structure factor calculations at idealized positions. Selected crystal data and structural refinement parameters are collected in Table 1.

Polymerization Procedures and Polymer Characterizations. All polymerizations with cationic titanium methyl complex **1** were performed in 25 mL, oven- and then flame-dried vacuum flasks inside an argon-filled glovebox. Separate stock solutions of $CGCTiMe_2$ and B(C_6F_5)$_3$ (9.34 mM in 50 mL toluene) were first prepared. In a typical procedure, $CGCTiMe_2$ (5.0 mL, 46.7 μmol) and B(C_6F_5)$_3$ (5.0 mL, 46.7 μmol) were mixed in the flask and stirred for 10 min to cleanly generate CGCTiMe$^+$MeB(C_6F_5)$_3^-$ (**1**). MMA (1.00 mL, 9.35 mmol) or BMA (1.48 mL, 9.35 mmol) was quickly added, and the flask was sealed. For block copolymerizations, a second quantity of MMA or BMA was added after the completion of the first block (9 h for MMA, 12 h for BMA), plus a 30 min delay, and the polymerization was continued. After the measured time interval, the flask was removed from the glovebox and quenched by adding 5 mL of 5% HCl-acidified methanol. The quenched mixture was precipitated into 100 mL of methanol, stirred for 1 h, filtered, and washed with methanol. The polymer collected was dissolved in 5 mL of methylene chloride, precipitated into 100 mL of methanol, filtered, and dried in a vacuum oven at 50 °C overnight to a constant weight. PMMA- and PMMA-

Table 2. MMA and BMA Homo- and Copolymerization Results by 1[a]

entry no.	polymer type	time (h)	yield (%)	10^3M_n(calcd)	10^3M_n(found)	PDI	T_g (°C)	[rr] (%)	[mr] (%)	[mm] (%)
1	PMMA	9	98	20.0	23.6	1.09	117	81.8	16.7	1.5
2	PBMA	12	98	28.4	31.7	1.12	38	89.0	11.0	0.0
3	PBMA	16	97	28.4	31.9	1.12		88.9	11.1	0.0
4	PMMA-b-PMMA	9.5−9.5	>99	40.1	41.2	1.08	129	81.1	17.2	1.7
5	PMMA-b-PBMA	9.5−12.5	>99	48.5	50.2	1.08	120	86.4	13.1	0.5
6	PBMA-b-PMMA	16−9.5	>99	48.5	50.9	1.09	38	84.9	14.6	0.5
7	PMMA-co-PBMA	24	>99	24.2	28.8	1.08	72	86.6	13.1	0.4

[a] $[monomer]_0/[\mathbf{1}]_0 = 200$ for entries 1−3 and 7; $[monomer]_0/[\mathbf{1}]_0 = 400$ for entries 4−6.

containing copolymers obtained are white powdery materials, whereas PBMA is a glassy solid.

For MMA polymerizations with CGC Ti ester enolate complexes, two different approaches—activated catalyst and activated monomer—were used. In the activated catalyst approach, $B(C_6F_5)_3$·THF and complex **4** were premixed in CH_2Cl_2 and stirred for 10 min to generate **5** in situ followed by addition of MMA to start the polymerization. In the activated monomer approach, $B(C_6F_5)_3$ and MMA were premixed in CH_2Cl_2 or toluene followed by addition of the neutral ester enolate initiator **4** to start the polymerization. The workup procedure was the same as the above-described polymerization procedure using complex **1**, except that the polymer after quenching and precipitation was not redissolved in CH_2Cl_2 and reprecipitated into methanol.

Glass transition temperatures (T_g) of the polymers were measured by differential scanning calorimetry (DSC) on a DSC 2920, TA Instrument. Samples were first heated to 180 °C at 10 °C/min, equilibrated at this temperature for 4 min, and cooled to −35 °C at 10 °C/min. After being held at this temperature for 4 min, the samples were then reheated to 180 °C at 10 °C/min. All T_g values were obtained from the second scan, after removing the thermal history. Polymer molecular weights and molecular weight distributions were measured by gel permeation chromatography (GPC) analyses carried out at 40 °C, at a flow rate of 1.0 mL/min, and with THF as the eluent, on a Waters University 1500 GPC instrument. The instrument was calibrated using 10 PMMA standards, and chromatograms were processed with Waters Empower software. ^1H and ^{13}C NMR spectra for the analysis of PMMA and PBMA microstructures were recorded in $CDCl_3$ and analyzed according to the literature.[23]

Results and Discussion

Living and Syndioselective Polymerization of Methacrylates by CGCTiMe$^+$MeB$(C_6F_5)_3^-$ (1). Evidence that polymerizations of MMA and BMA by **1** in toluene at ambient temperature proceed in a living, syndioselective fashion derives from several lines. *First*, the degree of polymerization control in the homopolymerization of MMA was demonstrated by a linear increase of number-average molecular weight (M_n) with an increase in monomer conversion and by a small, insensitive molecular weight distribution (PDI ranging from 1.08 to 1.09) to conversion (Figure 1). The PMMA obtained has a syndiotacticity of [rr] ∼ 82% (entry 1, Table 2). A deviation of the found M_n (23 600) from the calculated M_n (20 000) upon a quantitative monomer conversion is attributed to a small consumption of the highly sensitive **1** by the solvent or atmosphere (no scavengers or other additives were used in the current polymerization system).

Polymerization of BMA proceeds in the same controlled fashion, producing syndiotactic ([rr] ∼ 89%, Figure 2) and high T_g (38 °C) PBMA[24] (entry 2, Table 2). The stability of the living PBMA polymer chain at RT was also examined. After all the monomer was consumed, an extended reaction time (4 h) afforded virtually the same PBMA as the polymerization quenched immediately after the completion (entry 3 vs 2).

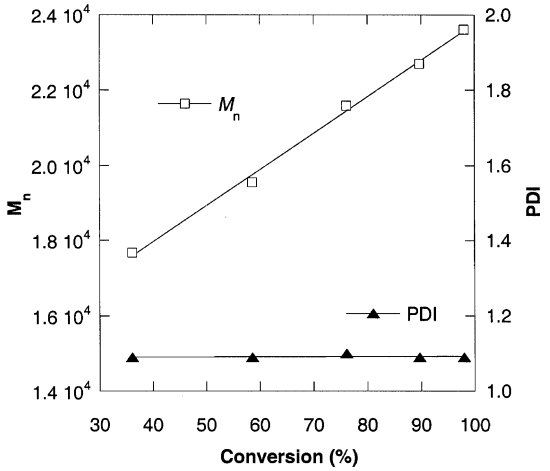

Figure 1. M_n and PDI of PMMA as a function of monomer conversion.

Second, reinitiation of a second 200 equiv of MMA—after the first 200 equiv of MMA had been consumed, plus a 30 min delay—approximately doubled M_n of PMMA, but PDI and syndiotacticity of PMMA did not change (entry 4 vs 1). The T_g (129 °C) of the PMMA from the reinitiation experiment is, however, 12 °C higher than that of the PMMA from the polymerization of the first 200 equiv MMA, reflecting a significant effect of M_n on T_g for relatively small molecular weight PMMA samples.

Third, sequential copolymerization of MMA and BMA starting from polymerization of MMA afforded well-defined block copolymer PMMA-*b*-PBMA, with M_n nearing the calculated value (entry 5) and a single sharp peak on the GPC trace (PDI = 1.08, Chart 1). The block copolymer PMMA-*b*-PBMA exhibits two distinct T_g's characteristic of each of the component segments (i.e, T_g (1) = 120 °C for the *s*-PMMA block and T_g (2) = 44 °C for the *s*-PBMA block). The molar composition of two monomer units in the block copolymer obtained from the ^1H NMR analysis (Figure 3) is the same as the monomer molar feed ratio (i.e., 1:1). The syndiotacticity of the block copolymer is collectively ∼86%; this is an overall value accounting for both blocks because of an overlap in the methyl triad region of PMMA and PBMA (Figure 3). However, the [rrrr] pentad in the C=O region by ^{13}C NMR can be resolved and distinguished for both blocks (Figure 4).

The well-defined block copolymer was also prepared from sequential copolymerization starting from polymerization of BMA. The PBMA-*b*-PMMA block copolymer obtained from this sequence is almost the same as PMMA-*b*-PBMA, except for a small variation in syndiotacticity and T_g (entry 6 vs 5). This experiment further confirms that both PMMA and PBMA polymer chains initiated by **1** are living under the conditions employed in this study.

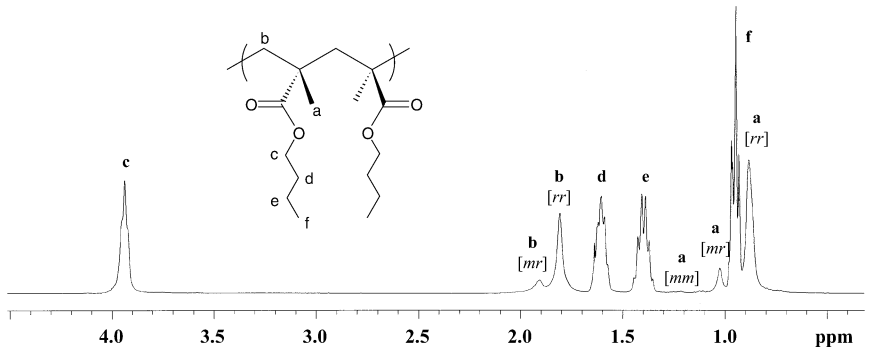

Figure 2. ^{1}H NMR spectrum ($CDCl_3$) of syndiotactic PBMA: methyl and methylene triads.

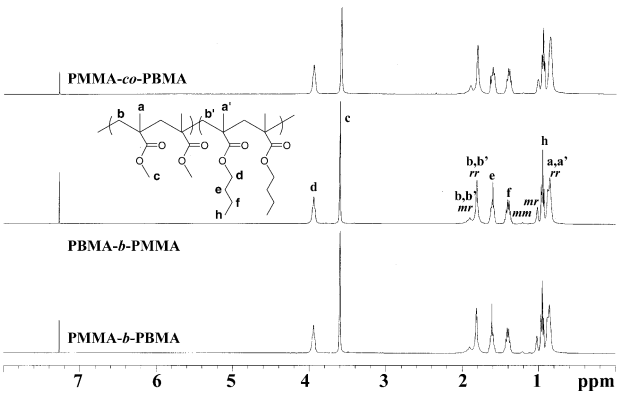

Figure 3. ^{1}H NMR spectra ($CDCl_3$) of block and random copolymers: nearly identical 1:1 MMA:BMA compositions and peak assignments.

Last, copolymerizing MMA and BMA simultaneously produced homogeneous random copolymer PMMA-*co*-PBMA (entry 7). The GPC trace shows a single sharp peak with PDI = 1.08 (Chart 1), and the NMR reveals an overall syndiotacticity of ~86%, which is similar to those of the block copolymers. A 1.1:1.0 MMA:BMA molar composition of two monomer units in the copolymer (Figure 3) is close to the monomer molar feed ratio (1:1) used for this copolymerization. As direct evidence for the formation of the homogeneous random copolymer, PMMA-*co*-PBMA displays a single T_g = 72 °C; this T_g compares well with a predicted value (68 °C) by the Fox equation ($1/T_g = W_1/T_g(1) + W_2/T_g(2)$) for random copolymers.[25]

Synthesis of CGC Ti Ester Enolates and Structure of CGCTiMe[OC(O^{i}Pr)═CMe$_2$] (4). Collins and co-workers showed that the cationic CGC Zr ester enolate, which was generated by in situ mixing of CGCZr[OC(O^{t}Bu)═CMe$_2$]$_2$ and [(Et$_2$O)$_2$H]$^+$[B(3,5-(CF$_3$)$_2$C$_6$H$_3$)$_4$]$^-$ at low temperatures, is active for MMA polymerization but produces isotactic PMMA via an enantiomorphic site control mechanism.[7d] However, in the case of cationic alkyl initiators, CGCTiMe$^+$MeB(C$_6$F$_5$)$_3^-$ promotes living and syndioselective MMA polymerization at ambient temperature (vide supra), whereas the isostructural Zr complex (i.e., CGCZrMe$^+$MeB(C$_6$F$_5$)$_3^-$) has no MMA polymerization activity under otherwise identical conditions. To better understand the diastereomeric PMMA formed by the CGC Ti and Zr initiators and compare the polymerization behavior of CGC cationic ester enolate initiators, the synthesis of neutral and cationic CGC Ti ester enolate complexes is needed.

Reaction of CGCTiCl$_2$ with lithium isopropylisobutyrate [Li(IPIB)] in THF or toluene readily produces CGCTiCl[OC(O^{i}Pr)═CMe$_2$] (**2**) as a microcrystalline orange red solid (Scheme 1). However, attempts to prepare the CGC Ti bis-enolate complex using up to 3 equiv of Li(IPIB) were unsuccessful; the mono-enolate **2** was always the product at all [Li(IPIB)]/CGCTiCl$_2$ ratios investigated (1−3), and there was no evidence for the formation of the bis-enolate species, presumably because the sterically crowded Ti center hinders the introduction of a second ester enolate ligand.

Scheme 1

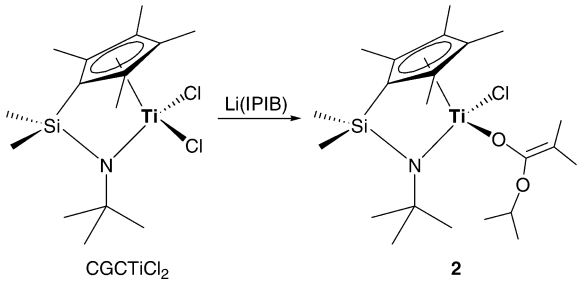

Direct methylation of **2** with either MeMgBr or MeLi gave a product mixture containing the anticipated methyl complex CGCTiMe[OC(O^{i}Pr)═CMe$_2$] (**4**) only as a minor product. A major (75% by NMR), unidentified product has nearly the same spectroscopic characteristics as those of **2** (i.e., C_1 symmetry and no Ti−Me moiety), but is definitely not **2**. Varying the reaction conditions (ratio, temperature, and solvent) did not result in any marked changes in the ratio of the products, and attempts to separate these two products by repeated recrystallization were unsuccessful. These experiments show that the route to **4** via direct methylation of **2** is not feasible.

In light of this finding, we realized that, for an effective synthesis of **4**, it is necessary to introduce the methyl group before the ester enolate ligand. Accordingly, CGCTiMeCl (**3**) was identified as a suitable precursor for this purpose. Attempts to prepare CGCTiMeCl using conventional methods, including reactions of CGCTiCl$_2$ with MeLi or AlMe$_3$ and of CGCTiMe$_2$ with Et$_3$NH$^+$Cl$^-$, gave inseparable mixtures containing CGCTiCl$_2$, CGCTiMe$_2$, and CGCTiMeCl. However, the reaction of the mono-enolate **2** with an excess of AlMe$_3$ cleanly produces **3** in an 89% isolated yield (Scheme 2). Subsequent reaction of **3** with Li(IPIB) produces CGCTiMe[OC(O^{i}Pr)═CMe$_2$] (**4**) in an 58% isolated yield (Scheme 2). Combining these two reactions into a "one-pot" reaction (i.e., without isolating intermediate **3**) also works with a much improved overall yield of **4** (81%), but it is necessary to remove any residue AlMe$_3$ before addition of Li(IPIB) in the second step because AlMe$_3$ further reacts with **4** to produce CGCTiMe$_2$.

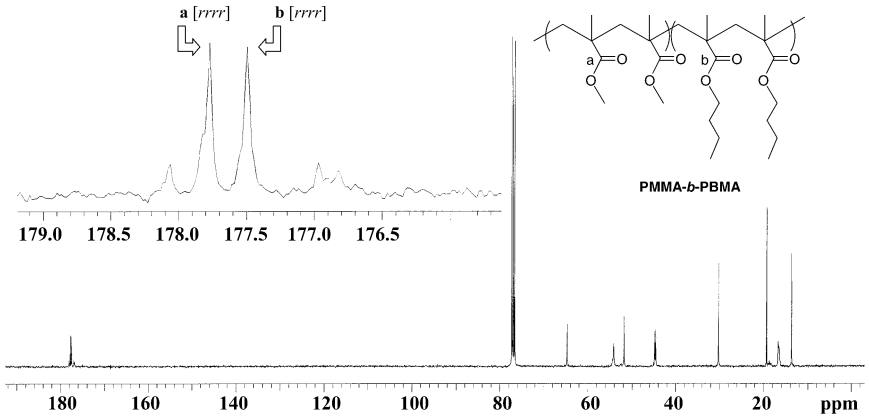

Figure 4. ^{13}C NMR ($CDCl_3$) spectrum of syndiotactic PMMA-*b*-PBMA: full spectrum and expanded pentad distributions in the C═O region.

Scheme 2

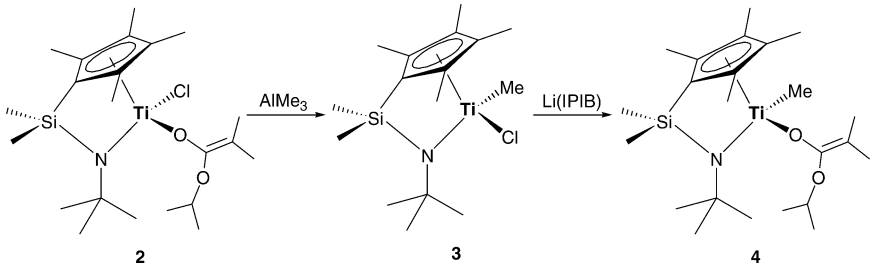

Table 3. Selected Bond Lengths (Å) and Bond Angles (deg) for 4

Ti−O(1)	1.826(2)	Ti−C(23)	2.131(4)
Ti−N	1.953(3)	Ti−Cp(centroid)	2.035
C(19)−O(1)	1.347(4)	C(19)−O(2)	1.377(4)
C(19)−C(20)	1.323(5)	C(16)−O(2)	1.443(4)
Ti−O(1)−C(19)	159.6(2)	O(1)−Ti−N	111.64(12)
O(1)−Ti−C(23)	100.69(13)	N−Ti−C(23)	105.19(14)
Cp(centroid)−Ti−N	107.7	O(1)−C(19)−C(20)	124.8(3)
O(1)−C(19)−O(2)	113.8(3)	O(2)−C(19)−C(20)	121.3(3)

The molecular structure of CGCTiMe[OC(O^{i}Pr)═CMe_2] (**4**) is shown in Figure 5; important bond lengths and angles are tabulated in Table 3. Of particular interest are a large Ti−O(1)−C(19) vector angle of 159.6(2)° and a short Ti−O(1) length of 1.826(2) Å. In Cp-based titanocene alkoxide, enolate, and carboxylate complexes, the Ti−O−C vector angles and the Ti−O lengths are in the ranges of 133−166° and 1.75−1.93 Å, respectively, reflecting various degrees of the $p_\pi-d_\pi$ interaction between oxygen and the electron-deficient titanium center.[26] In an analogous titanium ester enolate complex, $Cp_2TiCl\{OC(OMe)═CMe_2\}$,[27] this π-type

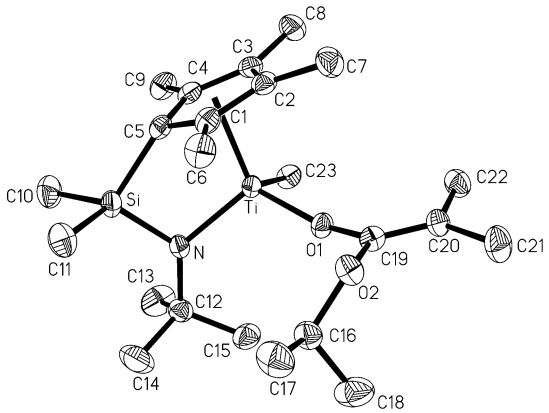

Figure 5. Molecular structure of **4**.

Ti−O interaction was considered relatively minor, as judged by a small Ti−O−C vector angle of 141.5(8)° and a Ti−O distance of 1.888(7) Å. In short, comparing the metric parameters in complex **4** with the literature values clearly indicates the partial double-bond character for the Ti−O(1) bond in **4**, where the oxygen is partly *sp*-hybridized.

The C(19)═C(20) double bond is characterized by a bond length of 1.323(5) Å and a sum of the angles around C(19) of 359.9° for a trigonal-planar geometry. A Cp(centroid)−Ti−N angle of 107.7° is identical to that of $CGCTiCl_2$,[17k] indicative of a constrained geometry about the Ti center.

MMA Polymerization by CGCTiCl[OC(O^{i}Pr)═CMe_2] (2), CGCTiMe[OC(O^{i}Pr)═CMe_2] (4), and [CGCTi$^+$(THF)[OC(O^{i}Pr)═CMe_2][$MeB(C_6F_5)_3$]$^-$ (5). Complex **2**, either by itself or in combination with activator $Li^+[B(C_6F_5)_4]^-$, is inactive for MMA polymerization in toluene, THF, or a toluene/THF mixture. Complex **4** by itself is also inactive for MMA polymerization; however, premixing MMA with $B(C_6F_5)_3$ in toluene followed by addition of **4** at a molar ratio of [MMA]/[$B(C_6F_5)_3$]/[**4**] = 200:1:1 produced PMMA in 62% isolated polymer yield in 9 h at ambient temperature. The PMMA formed has a $M_n = 3.06 \times 10^4$, a PDI of 1.14, and a syndiotacticity of [rr] = 77.1% ([mr] = 19.9%; [mm] = 2.9%). The same polymerization, but carried out in CH_2Cl_2, produced a similar polymer yield (60%) and polymer characteristics ($M_n = 2.93 \times 10^4$; PDI = 1.12; [rr] = 77.3%; [mr] = 19.6%; [mm] = 3.1%).

The primary interest here is to use the preformed cationic CGC Ti ester enolate for MMA polymerization studies. To this end, cationic CGC Ti ester enolate **5** is generated by in situ mixing of **4** and $B(C_6F_5)_3$·THF in methylene chloride (Scheme 3). The use of a stoichiometric amount of THF (from $B(C_6F_5)_3$·THF) is critical for the formation of the stable cationic ester enolate complex **5**; however, the product is not isolable, presum-

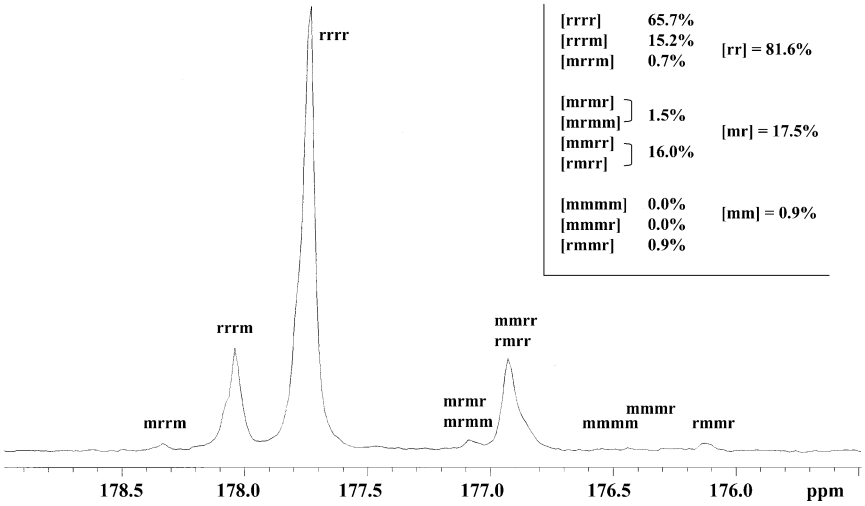

Figure 6. ^{13}C NMR ($CDCl_3$) spectrum of syndiotactic PMMA produced by **1** (entry 1, Table 2): pentad distributions in the C=O region.

Scheme 3

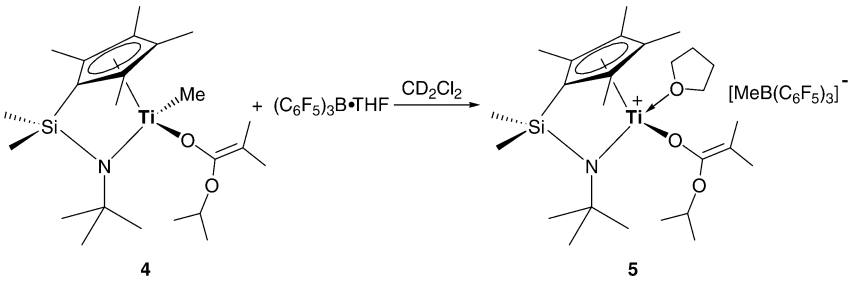

ably due to its poor thermal stability in the solid state. Nevertheless, the solution NMR spectral characteristics (see Experimental Section) are consistent with the structure of the cation **5**. Most notable are the disappearance of the sharp Ti−Me peak in **4**, the appearance of the broad B−Me peak in **5**, and the observed >0.1 and >0.3 ppm downfield shifts for the =C*Me*$_2$ and Si*Me*$_2$ methyl groups, respectively, on going from the neutral enolate **4** to the cationic enolate **5**. The chemical shift for the methyl group in the $[MeB(C_6F_5)_3]^-$ anion is 0.46 ppm in CD_2Cl_2, comparing well with that reported for the free $[MeB(C_6F_5)_3]^-$ anion.[28] The formation of the borate anion and its noncoordinating nature in **5** are also established by ^{19}F NMR spectra in which a small chemical shift difference of <3 ppm [$\Delta(m,p\text{-F})$ = 2.6 ppm in **5**] between the *para*- and *meta*-fluorines is diagnostic of the noncoordinating $[MeB(C_6F_5)_3]^-$ anion.[28,29]

Subsequently, the in situ generated cation **5** in methylene chloride at ambient temperature was used for MMA polymerization. Using methylene chloride as solvent and under conditions otherwise identical to those of the MMA polymerization by **1**, MMA polymerization by **5** produced PMMA having a $M_n = 2.71 \times 10^4$, a PDI = 1.12, and a syndiotacticity of [rr] = 80.0% ([mr] = 18.0%; [mm] = 2.0%). These polymer characteristics by **5** are remarkably similar to those by **1**, suggesting that the same propagating mechanism is operative for both initiators and that the cationic CGC Ti ester enolate **5** is an appropriate model for the propagating species involved in the MMA polymerization by **1**.

Microstructures and Mechanism. The triad-level microstructure of the PMMA by both **1** and **5** is more characteristic of chain-end control than site control, but the microstructure did not conform to pure chain-end control. A triad test using 4[mm][rr]/[mr]^2 gave 1.76 and 1.98 for PMMA by **1** and **5**, respectively, both deviating significantly from unity for a pure chain-end control mechanism. It should be noted that this is a very sensitive test and may not be suitable for the analysis of the microstructure where [mm] or [rr] is small.[23a] Accordingly, a Bernoulli statistic model was also tested using the sum of two probabilities: $P_{m/r}$ and $P_{r/m}$.[23a] This test gave $P_{m/r} + P_{r/m} = 0.94$ for PMMA by **1** and $P_{m/r} + P_{r/m} = 0.92$ for PMMA by **5** for predominant chain-end control, but still noticeably deviating from Bernoullian statistics (i.e., $P_{m/r} + P_{r/m} \neq 1.0$).

To examine if this deviation is due to the unsuitability of analyzing triads for polymers with small [mm] or [rr] values or if other models may apply, we analyzed the microstructure of the PMMA by **1** at the pentad level (Figure 6). It should be pointed out that one cannot use a ratio of [rrrm]/[rrmr] = 1.00 for testing a chain-end control mechanism because two pentads, rrmr and mmrr, are inseparable in ^{13}C NMR for PMMA. However, with now accurate triad distributions deduced from the pentads, we recalculated the two probabilities: $P_{m/r} = 0.907$ and $P_{r/m} = 0.096$, the sum of which gave $P_{m/r} + P_{r/m} = 1.003$ for pure chain-end control. The trials to fit the pentads to other models such as the penultimate Markov and two-state Coleman−Fox[30] models using literature methods[23a] yielded less conformity; therefore, the chain-end control mechanism is concluded to be responsible for the resulting microstructure.

The isostructural, cationic CGC Zr ester enolate initiator produces highly isotactic PMMA via a site control mechanism at low temperatures.[7d] A key element in the proposed mechanism is one-site monomer

addition; that is, C−C bond formation (by monometallic, 1,4-conjugated Michael addition) occurs predominantly via the same, "locked" conformation imposed by slow dissociation of the terminal ester group (relative to associative displacement by MMA) and fast Michael addition (relative to racemization at Zr by exchange of free and bound MMA). In the case of the more sterically crowded Ti initiator, dissociation of the terminal ester group after each C−C bond formation is likely fast; the inability to introduce a second bulky ester enolate ligand to the CGC Ti center (vide supra) supports this point. Accordingly, alternating MMA addition at both lateral coordination sites is proposed for the Ti initiator, under which mechanism and CGC ligation syndiotactic PMMA should be formed. However, the chain-end control characteristic of the polymerization by the apparently chiral initiator **1** or **5** suggests racemization at Ti (by exchanging free and bound MMA) is rapid compared to the rate of propagation; the observation of no polymerization activity for **5** at temperatures below 0 °C indicates a higher activation barrier for MMA addition by **5** than that by the isostructural Zr initiator, whereas the observed time-average C_s-symmetry of **5** in THF-d_8 at room temperature shows rapid racemization at Ti. A possibility of a bimetallic mechanism for cationic initiator **1** or **5** would require bringing two *cationic* Ti centers in proximity for cross Michael addition involving two cationic Ti centers; this is perhaps a less energetically favored pathway, although in this fashion mixed chain-end and site control mechanisms are possible, where their interplay might also explain the microstructure of the PMMA formed by **1** or **5**.

In conclusion, unlike the isostructural, cationic CGC Zr alkyl complex (i.e., $CGCZrMe^+MeB(C_6F_5)_3^-$), which is inactive for polymerization of methacrylates, the cationic Ti alkyl complex **1** effects living and syndioselective polymerizations of MMA and BMA at ambient temperature, allowing for the first synthesis of the well-defined, syndiotactic block or random copolymers of methacrylates using a cationic titanium complex. Furthermore, unlike the isostructural, cationic CGC Zr ester enolate complex, which produces *isotactic* PMMA via enantiomorphic site control, the cationic Ti ester enolate complex **5** produces *syndiotactic* PMMA via chain-end control. The current finding—Ti complexes behave drastically different from those of the isostructural Zr complexes in polymerization of methacrylates—points to the significant effect of metal on metallocene-mediated methacrylate polymerization activity and stereoregulation.

Acknowledgment. We thank Susie M. Miller for determination of the crystal structure, Andrew D. Bolig for the preparation of lithium isopropylisobutyrate, Boulder Scientific Co. for the gift of $B(C_6F_5)_3$, and Dr. David R. Wilson of Dow Chemical for the gift of $CGCTiCl_2$. E.Y.-X.C. gratefully acknowledges an Alfred P. Sloan Research Fellowship.

Supporting Information Available: Crystallographic data for **4** (CIF). This material is available free of charge via the Internet at http://pubs.acs.org.

References and Notes

(1) Farnham, W. B.; Hertler, W. U.S. Pat. 4,728,706, 1988.
(2) Yasuda, H.; Yamamoto, H.; Yokota, K.; Miyake, S.; Nakamura, A. *J. Am. Chem. Soc.* **1992**, *114*, 4908−4909.
(3) Collins, S.; Ward, S. G. *J. Am. Chem. Soc.* **1992**, *114*, 5460−5462.
(4) (a) Li, Y.; Ward, D. G.; Reddy, S. S.; Collins, S. *Macromolecules* **1997**, *30*, 1875−1883. (b) Collins, S.; Ward, D. G.; Suddaby, K. H. *Macromolecules* **1994**, *27*, 7222−7224.
(5) (a) Sogah, D. Y.; Hertler, W. R.; Webster, O. W.; Cohen, G. M. *Macromolecules* **1987**, *20*, 1473−1488. (b) Webster, O. W.; Hertler, W. R.; Sogah, D. Y.; Farnham, W. B.; RajanBabu, T. V. *J. Am. Chem. Soc.* **1983**, *105*, 5706−5708.
(6) Bandermann, F.; Ferenz, M.; Sustmann, R.; Sicking, W. *Macromol. Symp.* **2001**, *174*, 247−253.
(7) (a) Bolig, A. D.; Chen, E. Y.-X. *J. Am. Chem. Soc.* **2002**, *124*, 5612−5613. (b) Frauenrath, H.; Keul, H.; Höcker, H. *Macromolecules* **2001**, *34*, 14−19. (c) Hölscher, M.; Keul, H.; Höcker, H. *Chem.—Eur. J.* **2001**, *7*, 5419−5426. (d) Nguyen, H.; Jarvis, A. P.; Lesley, M. J. G.; Kelly, W. M.; Reddy, S. S.; Taylor, N. J.; Collins, S. *Macromolecules* **2000**, *33*, 1508−1510. (e) Deng, H.; Shiono, T.; Soga, K. *Macromolecules* **1995**, *28*, 3067−3073.
(8) Yasuda, H.; Yamamoto, H.; Yamashita, M.; Yokota, K.; Nakamura, A.; Miyake, S.; Kai, Y.; Kanehisa, N. *Macromolecules* **1993**, *26*, 7134−7143.
(9) Batis, C.; Karanikolopoulos, G.; Pitsikalis, M.; Hadjichristidis, N. *Macromolecules* **2003**, *36*, 9763−9774.
(10) Cameron, P. A.; Gibson, V.; Graham, A. J. *Macromolecules* **2000**, *33*, 4329−4335.
(11) Simionescu, C.; Asandei, N.; Benedek, I.; Ungureanu, C. *Eur. Polym. J.* **1969**, *5*, 449−462.
(12) Saegusa, N.; Shiono, T.; Ikeda, T.; Mikami, K. JP 10330391, 1998.
(13) Jensen, T. R.; Yoon, S. C.; Dash, A. K.; Luo, L.; Marks, T. J. *J. Am. Chem. Soc.* **2003**, *125*, 14482−14494.
(14) Spaether, W.; Klass, K.; Erker, G.; Zippel, F.; Fröhlich, R. *Chem. Eur. J.* **1998**, *4*, 1411−1417.
(15) (a) Jin, J.; Mariott, W. R.; Chen, E. Y.-X. *J. Polym. Chem., Part A: Polym. Chem.* **2003**, *41*, 3132−3142. (b) Jin, J.; Chen, E. Y.-X. *Organometallics* **2002**, *21*, 13−15.
(16) Jin, J.; Chen, E. Y.-X. *Macromol. Chem. Phys.* **2002**, *203*, 2329−2333.
(17) For selected examples, see: (a) Xu, Z.; Vanka, K.; Ziegler, T. *Organometallics* **2004**, *23*, 104−116. (b) Okuda, J. *Dalton Trans.* **2003**, 2367−2378. (c) Li, L.; Metz, M. V.; Li, H.; Chen, M.-C.; Marks, T. J.; Liable-Sands, L.; Rheingold, A. L. *J. Am. Chem. Soc.* **2002**, *124*, 12725−12741. (d) Kunz, K.; Erker, G.; Kehr, G.; Fröhlich, R.; Jacobsen, H.; Berke, H.; Blacque, O. *J. Am. Chem. Soc.* **2002**, *124*, 3316−3326. (e) Carpentier, J.-F.; Maryin, V. P.; Luci, J.; Jordan, R. F. *J. Am. Chem. Soc.* **2001**, *123*, 898−909. (f) Chen, E. Y.-X.; Kruper, W. J.; Roof, G.; Wilson, D. R. *J. Am. Chem. Soc.* **2001**, *123*, 745−746. (g) Lanza, G.; Fragalà, I. L.; Marks, T. J. *J. Am. Chem. Soc.* **2000**, *122*, 12764−12777. (h) Chum, P. S.; Kruper, W. J.; Guest, M. J. *Adv. Mater.* **2000**, *12*, 1759−1767. (i) McKnight, A. L.; Waymouth, R. M. *Chem. Rev.* **1998**, *98*, 2587−2598. (j) Devore, D. D.; Timmers, F. J.; Hasha, D. L.; Rosen, R. K.; Marks, T. J.; Deck, P. A.; Stern, C. L. *Organometallics* **1995**, *14*, 3132−3134. (k) Stevens, J. C. In *Catalyst Design for Tailor-Made Polyolefins*; Soga, K., Terano, M., Eds. *Stud. Surf. Sci. Catal.* **1994**, *89*, 277−284. (l) Shapiro, P. J.; Cotter, W. D.; Schaefer, W. P.; Labinger, J. A.; Bercaw, J. E. *J. Am. Chem. Soc.* **1994**, *116*, 4623−4640. (m) Okuda, J. *Comments Inorg. Chem.* **1994**, *16*, 185−205. (n) Canich, J. A. Eur. Pat. Appl. EP 0 420 436 A1, 1991. (o) Stevens, J. C.; Timmers, F. J.; Wilson, D. R.; Schmidt, G. F.; Nickias, P. N.; Rosen, R. K.; Knight, G. W.; Lai, S. Eur. Pat. Appl. EP 0 416 815 A2, 1991. (p) Okuda, J. *Chem. Ber.* **1990**, *123*, 1649−1651. (q) Shapiro, P. J.; Bunel, E.; Schaefer, W. P.; Bercaw, J. E. *Organometallics* **1990**, *9*, 847−869. (r) Piers, W. E.; Shapiro, P. J.; Bunel, E.; Bercaw, J. E. *Synlett.* **1990**, *2*, 74−84.
(18) For a preliminary report of this subject, see: Chen, E. Y.-X.; Mariott, W. R. *Polym. Prepr. (Am. Chem. Soc., Div. Polym. Chem.)* **2004**, *45*, 993−994.
(19) Allen, R. D.; Long, T. E.; McGrath, J. E. *Polym. Bull.* **1986**, *15*, 127−134.
(20) Chen, Y.-X.; Marks, T. J. *Organometallics* **1997**, *16*, 3649−3657.
(21) Kim, Y.-J.; Bernstein, M. P.; Galiano Roth, A. S.; Romesberg, F. E.; Williard, P. G.; Fuller, D. J.; Harrison, A. T.; Collum, D. B. *J. Org. Chem.* **1991**, *56*, 4435−4439.
(22) Sheldrick, G. M. *SHELXTL*, Version 5; Siemens: Madison, WI, 1996.
(23) (a) Bovey, F. A.; Mirau, P. A. *NMR of Polymers*; Academic Press: San Diego, CA, 1996. (b) Chujo, R.; Hatada, K.; Kitamaru, R.; Kitayama, T.; Sato, H.; Tanaka, Y. *Polym. J.*

1987, *19*, 413−424. (c) Ferguson, R. C.; Ovenall, D. W. *Macromolecules* **1987**, *20*, 1245−1248. (d) Moad, G.; Solomon, D.; Spurling, T. H.; Johns, S. R.; Willing, R. I. *Aust. J. Chem.* **1986**, *39*, 43−50. (e) Ferguson, R. C.; Ovenall, D. W. *Polym. Prepr. (Am. Chem. Soc., Div. Polym. Chem.)* **1985**, *26*, 182−183. (f) Subramanian, R.; Allen, R. D.; McGrath, J. E.; Ward, T. C. *Polym. Prepr. (Am. Chem. Soc., Div. Polym. Chem.)* **1985**, *26*, 238−240.

(24) Typical syndiotactic PBMA has $T_g \sim 21$ °C; see: *Polymer Handbook*, 4th ed.; Brandrup, J., Immergut, E. H., Grulke, E. A., Eds.; Wiley: New York, 1999.

(25) Fox, T. G. *Bull. Am. Phys. Soc.* **1956**, *1*, 123.

(26) Curtis, M. D.; Thanedar, S.; Butler, W. M. *Organometallics* **1984**, *3*, 1855−1859.

(27) Hortmann, K.; Diebold, J.; Brintzinger, H.-H. *J. Organomet. Chem.* **1993**, *445*, 107−109.

(28) Klosin, J.; Roof, G. R.; Chen, E. Y.-X.; Abboud, K. A. *Organometallics* **2000**, *19*, 4684−4686.

(29) Horton, A. D.; de With, J.; van der Linder, A. J.; van de Weg, H. *Organometallics* **1996**, *15*, 2672−2674.

(30) We thank the reviewer for bringing this possibility to our attention.

MA049774G